Synergistic Noncovalent Catalysis Facilitates Base-Free Michael Addition

Synergistic Non-Covalent Catalysis Facilitates Base-Free Michael Addition

Jianzhu Wang,[†] Tom A. Young,[‡] Fernanda Duarte[‡]* and Paul J. Lusby[†]*

[†]EaStCHEM School of Chemistry, University of Edinburgh, Joseph Black Building, David Brewster Road, Edinburgh, Scotland, EH9 3FJ, U.K.

[‡] Chemistry Research Laboratory, University of Oxford, Mansfield Road, Oxford, OX1 3TA, U.K.

ABSTRACT: Carbon-Carbon bond forming processes that involve the deprotonation of a weakly acidic C-H pro-nucleophile using a strong Brønsted base are central to synthetic methodology. Enzymes also catalyze C-C bond formation from weakly C-H acidic substrates, however, they accomplish this at pH 7 using only collections of non-covalent interactions. Here we show that a simple, bio-inspired synthetic cage catalyzes Michael addition reactions using only coulombic and other weak interactions to activate various pro-nucleophiles and electrophiles. The anion-stabilizing property of the cage promotes spontaneous pro-nucleophile deprotonation, suggesting acidity-enhancement equivalent to several pK_a units. Using a second non-covalent reagent – commercially available 18-crown-6 – facilitates catalytic base-free addition of several challenging Michael partners. The cage's microenvironment also promotes high diastereoselectivity compared to a conventional base-catalyzed reaction.

Introduction

The organization of charge within an active site, which selectively stabilizes intermediates and transition states using electrostatic forces, is the basis for highly efficient enzyme catalysis.[1] This mode of reactivity provides a blueprint for developing synthetic catalysts that use only non-covalent interactions.[2] Self-assembled coordination cages are prime candidates for mimicking biological catalysts because (i) they provide a well-defined microenvironment that is distinct from the bulk phase and (ii) they invariably possess well defined, permanent charge. These facets have been beautifully demonstrated by Raymond, Bergman and Toste on numerous occasions, who have used a dodeca-anionic gallium tetrahedron to catalyze reactions that involve various cationic intermediates, such as oxonium[3] and iminium species,[4] carbocations[5] and positively-charged transition metal complexes.[6]

Anionic coordination cages are relatively rare compared to the vast number of cationic coordination assemblies that are built from transition metal ions and neutral ligands.[7] It seems somewhat surprising then that reports of catalysis that involve the stabilization of reactive anionic species within cationic cages are exceedingly rare.[8] There are several possible explanations for this apparent anomaly. Many cationic cage-compounds are effective hosts because they bind apolar substrates in water using the hydrophobic effect, while the associated anions are strongly hydrated and loosely associated with the cage-periphery.[8d] Anionic intermediates, unlike their cationic equivalents, can also be strongly coordinating and thus have the potential to disrupt the cage structure. Finally, anionic intermediates – again unlike cations – are also likely to be less well stabilized by the flat aromatic surfaces that define the cavity of a typical coordination cage. It should be noted, however, that highly deficient aromatic systems can be used to achieve catalysis by the stabilization of negatively charged intermediates, as exemplified by the elegant work of Matile using organo-naphthodiimide and C_{60} structures.[9] While it is difficult to identify the precise reasons for the lack of anion-stabilizing processes, what is clear is that being able to realize this apparently simple concept could open up the field of cage catalysis to a raft of new transformations, not least considering the plethora of C-C bond forming reactions that involve the deprotonation of weakly acidic C-H compounds. We now demonstrate the full effectiveness of this approach, using a simple cationic host system to catalyze Michael addition with remarkable efficiency.

Results and Discussion

We have previously shown that simple Pd_2L_4 coordination cages,[7d-h] like **C1** and **C2** (Figure 1a), can act as highly efficient catalysts.[10a-c] The catalytic properties of these cages do not stem from entropic effects, such as the dual encapsulation[11a-c] or constrictive binding mechanisms[11d] that have dominated earlier bio-inspired approaches. Instead, the activity of **C1** and **C2** arises because they can enthalpically stabilize polar intermediates and transition states (TS). This stabilization is facilitated by using large non-coordinating BArF counteranions, which are unable to access the cavity and leaves a charge-dense interior that is coulombically frustrated. Furthermore, the cationic Pd ions polarize the adjacent C-H bonds, creating pockets of H-bond donor atoms (Figure 1a, shown in blue) that can provide additional interactions. The BArF counteranions also impart solubility in apolar solvents, such as dichloromethane, leading to a poorly solvated inner microenvironment, further increasing the recognition of polar, reactive intermediates. Conversely, traditional small non-coordinating anions such as BF_4, PF_6 and OTf bind tightly inside the cage, especially in apolar solvents, which significantly reduces the affinity towards other species.[10d]

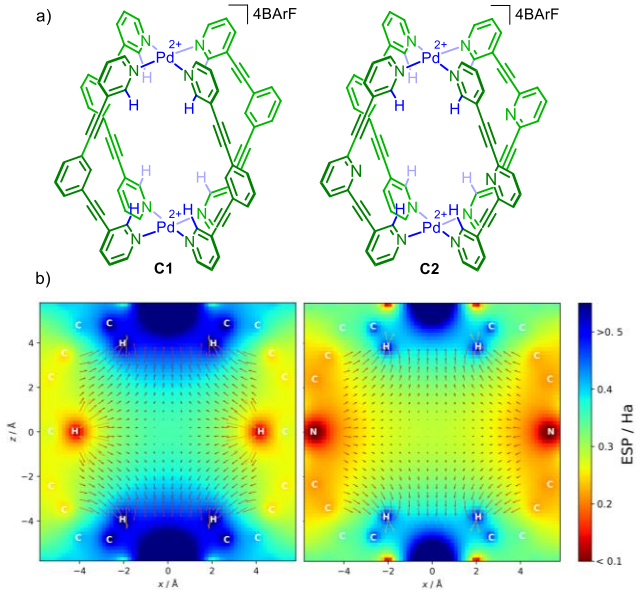

Figure 1. (a) Chemical structure of non-covalent Michael addition cage catalysts. The large, non-coordinating BArF counteranions create a highly polar, coulombically-frustrated cavity that can provide significant reactive intermediate and transition state stabilization. **(b) Electrostatic potential (ESP) slices of cages C1 and C2 on the xz plane containing two opposing ligands and the two metal centers.** Positive values (red) indicate increases in the electron density, while negative values (blue) indicate electron density reductions. Arrows represent the electric field defined from negative to positive (∇ESP) where the length corresponds to the magnitude.

Despite the similarity in the chemical structures of **C1** and **C2**, the two cages show quite distinct catalytic properties. **C2** shows excellent activity for Diels-Alder reactions with quinone dienophiles,[10a] which are bound strongly as the two carbonyl oxygen atoms are matched to interact simultaneously with both H-bond donor pockets. This catalysis shows selective TS stabilisation that is comparable to the most active catalytic antibody.[10a] In contrast, **C1** is completely inactive – despite being able to bind quinones more strongly than **C2**. Calculations show that the different catalytic behaviour stems from the greater flexibility of **C2**.[10b] The surprisingly distinct properties are also manifest in the way the cages alter the redox properties of bound guests – but this time in reverse: **C1** is able to increase the reduction potential of bound quinones by as much as 1 V, corresponding to 90 kJ mol^{-1} radical-anion stabilization energy. These redox enhancing properties have been used to achieve electron transfer with non-bound substrates, generating radical-cation reactivity outside the cage.[9c] This time **C2** shows no activity. Electrostatic potential energy slices of the two cages (Figure 1b) reveal why **C2** is inferior at stabilising anionic species; the central non-coordinating nitrogen atoms significantly neutralize the potential, both centrally within the cavity and also at the distal Pd sites and H-bond donor atoms. It was therefore clear that **C1** should be the favoured choice for investigating reactions that involve encapsulated closed-shell anionic intermediates.

Michael addition was chosen as a representative reaction as it was expected that a bound quinone would act as an activated enone. External, intermolecular attack by a non-bound anioinic nucleophile would then generate a cage-stabilized oxyanion intermediate. Subsequent turnover would then involve the entropically neutral displacement of a single product by a single substrate, an approach we had successfully utilized to avoid product inhibition with DA catalysis.[10a] However, the reaction of 20 mol% **C1**, with either benzoquinone (K_a = 8000 M^{-1})[10d,e] or naphthoquinone (K_a = 3.5×10^5 M^{-1})[10d], and the relatively acidic yet weakly binding pro-nucleophile, nitromethylacetate, **Nu1**H ($K_a \approx 30$ M^{-1}), both in the absence and presence of non-coordinating base, DBU (1,8-Diazabicyclo[5.4.0]undec-7-ene, 10 mol%), gave no clear evidence of Michael addition product formation (Scheme 1a) instead only small quantities of unidentifiable products. Other cage-complementary electrophiles, such as dimethyl maleate (K_a = 1100 M^{-1}) also showed no formation of Michael adduct. While it was perhaps unsurprising that no reaction occurred in the absence of base, the lack of reaction between what we presumed would be a strongly bound, activated enone and the nucleophilic **Nu1**$^-$ was more disappointing. A closer examination of the ^{1}H NMR spectra, particularly for the reaction of dimethyl maleate (Figure S61), gave some clues as to the lack of reactivity. Specifically, on the addition of base to **C1**, **Nu1**H and dimethyl maleate, a second set of cage peaks appear while the dimethyl maleate electrophile shifts back towards the free-state. The appearance of a second set of cage peaks indicates the formation of a slowly exchanging species, which we infer to be the strongly bound nucleophilic anion complex, **Nu1**$^-$⊂**C1**. Hence, the deprotonated nucleophile simply displaces the bound electrophile rather than adding to the 1,4-position. The strategy of using a cage-complementary electrophile and a second much weaker binding nucleophile (to ensure turnover) was then reversed, using β-dicarbonyl pro-nucleophiles that are matched for **C1** (Scheme 1b). With this strategy, we thought that the use of a smaller electrophile, vinyl methyl ketone, **E1** (K_a < 30 M^{-1}), would aid access to the bound nucleophilic anion. This approach also showed no evidence of Michael addition products. The spectroscopic data for these reactions again indicated that the bound nucleophilic anion is generated but that this is simply unreactive. This is particularly clear for the reaction of Meldrum's acid with **E1**. In this case, the cage actually inhibits the reactivity that is seen with substrates and base only (Figures S65 and S66).

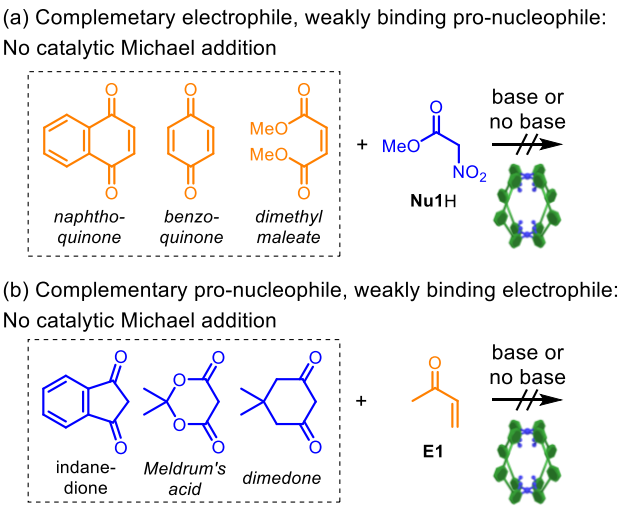

Scheme 1: Single-substrate binding approaches give no catalytic Michael addition. Dicarbonyl electrophiles and pro-nucleophiles (shown in dashed box bind) are a match for the H-bond donor sites of **C1**.

In light of these results, we extended our screen of reactions to a more diverse pairing of substrates, specifically the combined use of weakly binding **Nu1**H and **E1** (Scheme 2a). When these reactants were mixed with **C1** in dichloromethane, we were pleasantly surprised that the formation of product **P1** occurs even in the absence of an external base (Scheme 2b, blue squares). In contrast, the substrates only do not react under the same conditions (Scheme 2b, red diamonds) even after a week. Several control reactions have been carried out to confirm that reactivity stems from the cage's inner microenvironment (Scheme 2c). Adding the strong binding inhibitor pentacenedione ($K_a \approx 10^8$ M^{-1}) to the catalyzed process completely halts activity. The representative mononuclear complex, $[Pd(pyridine)_4](BArF)_2$, also shows no reactivity. Collectively, these results show **C1** is not simply serving as a source of Lewis acidic free Pd^{2+} ions or Brønsted basic pyridine groups and that catalysis is dependent on the substrates being able to access the cage cavity. We have also found that **C2** shows no reactivity under the same conditions. This provides further evidence that the highly homologous cages possess quite different properties, with **C1** favouring processes that involve bound anionic species.

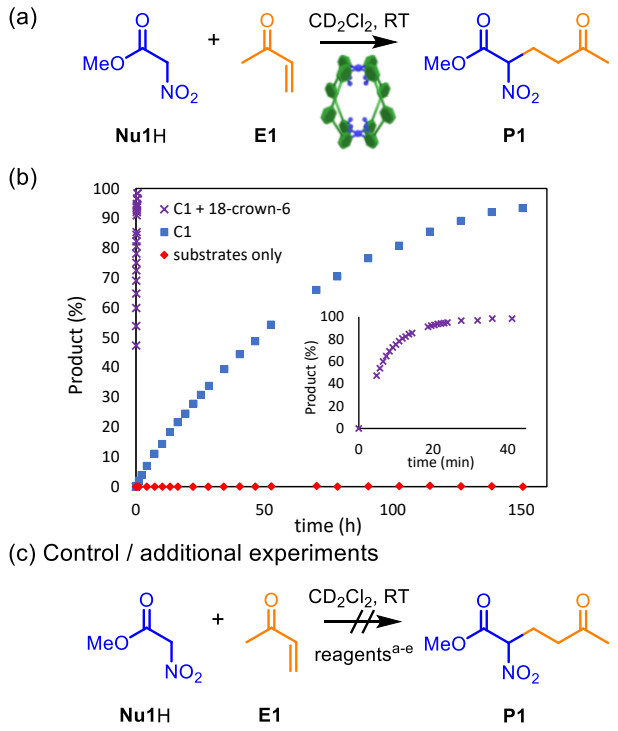

[a]**C1** + pentacenedione (Inhibitor, $K_a = 10^8$ M^{-1}); [b]$[Pd(pyridine)_4](BArF)_2$; [c]**C2**; [d]18-crown-6 only; [e]$[Pd(pyridine)_4](BArF)_2$ + 18-crown-6

Scheme 2: Base-free Michael addition catalysis. General reaction conditions: **C1** (0.5 mM, 20 mol%), **Nu1**H (12.5 mM), **E1** (2.5 mM), 18-crown-6 (2.5 mM), CD_2Cl_2, RT.

The reactivity of **C1** is remarkable considering its chemical structure (Figure 1a): it does not possess the Brønsted base functionality present in small molecule H-bond catalysts[12] nor any Lewis acid site, which makes it distinct from base-free transition metal systems.[13] The control experiment with $[Pd(pyridine)_4](BArF)_2$ further indicates that this functionality does not arise under experimental conditions due to the dissociation of components. In the absence of an obvious Brønsted base, it is likely that residual water elicits the deprotonation of **Nu1**H.[14] It is interesting to note the difference in pK_a of **Nu1**H and H_3O^+, which are +5.7 and −1.7, respectively.[15] These values are measured in water, therefore, a direct comparison to the non-aqueous system described here must be treated with caution. Nonetheless, it is clear that the cage significantly increases the acidity of the pro-nucleophile.[16] This large shift occurs because the tetrcatioinic cage is excellent at stabilizing the nucleophile conjugate anion, **Nu1**$^-$, through a mixture of coulombic and H-bond interactions. This large increase in acidity parallels recent redox studies, which showed that **C1** shifts the 1 e^- reduction potential by 1 V, presumably due to similar stabilization effects.[10c]

Expanding the substrate scope, we found that the similar pro-nucleophile benzoylnitromethane, **Nu2**H, also reacts with **E1** to generate Michael product **P2** quantitatively after 4.5 days (Scheme 3). Attempts to further widen the substrate scope to less acidic pro-nucleophiles and different Michael acceptors, however, showed minimal reactivity. We therefore reasoned that perhaps the limiting factor was not the stability of the nucleophile$^-$⊂**C1** host-guest complex, but rather the hydronium BArF species that is released from the reaction of water with the pro-nucleophile⊂**C1**. While hydronium is more likely to exist as a slightly more stable protonated water cluster, the bulk apolar solvent and non-coordinating BArF counteranion still make this a high energy species. In order to stabilize the hydronium ion, we postulated that commercially available 18-crown-6 could play this role.[17] We were thus delighted to find that when one equivalent of 18-crown-6 was added to the transformation of **Nu1**H and **E1** to give **P1**, a dramatic reduction in reaction time was observed, from several days with **C1** only to less than 40 min with crown ether additive (Scheme 2b, purple crosses). The control reaction with only 18-crown-6 and substrates gave no reactivity over several days (Scheme 2c), showing that synergistic non-covalent stabilization of the charge separated state is necessary. A further control experiment with the representative mononuclear complex $[Pd(pyridine)_4](BArF)_2$ and 18-crown-6 (Scheme 2c) also showed no reaction. With this control reaction, significant degradation of the mononuclear complex is observed, which again indicates that partial destruction releasing free components (e.g. Lewis acidic Pd^{2+} ions and pyridine base) is not responsible for catalysis. Notably, **C1** does not show any indication of decomposition in the presence of 18-crown-6, highlighting that the cage topology additionally imparts structural stability, presumably due to cooperative chelate effects. It is also worth noting that **C2** does show some reactivity with 18-crown-6, although much diminished compared to **C1** (See Figure S8), highlighting their differences are not dualistic.

We have also applied the **C1** / 18-crown-6 conditions to a preparative scale reaction to demonstrate the efficiency and simplicity of the method. In this instance, the loading of **C1** and 18-crown-6 can be lowered to 2 and 10 mol%, respectively – without any appreciable drop in yield (72 mg isolated yield, 91%, 2 days). The catalytic use of 18-crown-6 is also consistent with it binding a quantity of released H_3O^+ that is equal or less than the mol% of **C1** (assuming the affinity of crown-ether for hydronium is sufficiently high).

Armed with this combined non-covalent method, we turned to a wider scope (Scheme 3) of both different electrophiles (**E2-4)** and pro-nucleophiles (**Nu3-5**H). Methyl acrylate, **E2**, is seen as a challenging electrophile, much less reactive and difficult to activate than **E1** yet product **P3** is generated in excellent yield under catalytic conditions. Also, products **P3** to **P5**

demonstrate that the cage can activate electrophiles with a range of different functional groups. This functional group tolerance also applies to different pro-nucleophiles, with nitrile containing **Nu4**H and **Nu5**H giving products **P7** and **P8**, also in excellent yields. It is also worth noting that pro-nucleophiles **Nu3**-**5**H are significantly less acidic than either **Nu1**H or **Nu2**H, based on their reported pK_a values (≈ 10-11), further highlighting the remarkable acidification "power" of this combined non-covalent catalytic method.

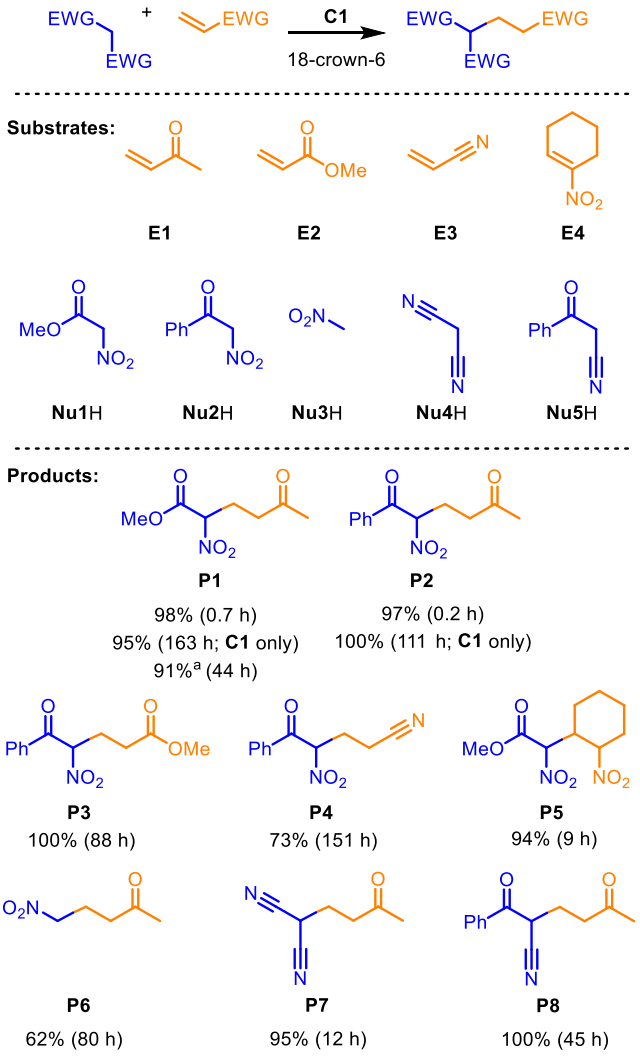

Scheme 3. Substrate scope for synergistic base-free Michael Addition catalysis. Conditions: 0.5 mM **C1**, 2.5 mM 18-crown-6, 2.5 mM electrophile, 12.5 mM pro-nucleophile, CD_2Cl_2, RT. Yield determined by ^{1}H NMR spectroscopy. [a]Isolated yield using **E1** (0.42 mmol), **NuH1** (0.63 mmol), **C1 (**8.4 µmol, 2 mol%) and 18-crown-6 (42 µmol, 10 mol%), CH_2Cl_2 (70 mL), RT, 44 h.

It has been revealing to compare this bio-inspired cage catalysis to small molecule non-covalent approaches. Quite surprisingly, we could find no reports of catalytic methods for generating products **P2-8**. However, the catalytic formation of **P1** under similar conditions has been described. The sub-stoichiometric use of organic-soluble bases (e.g. DABCO, NMP, NMI, DBU) under similar conditions (e.g. 10 mol% cat, chloroform, 60 °C, 18 h) have been used to give **P1** in quantitative yield.[18a] Also a bifunctional Brønsted base-hydrogen bond catalyst (quinine-squaramide) also mediates the formation of **P1** (2 mol% cat, toluene, RT, 4 h).[18b] Significantly, however, these small molecule non-covalent approaches use *ca*. two orders of magnitude higher concentrations compared to the **C1** / 18-crown-6 system.[12,18] To make a more accurate evaluation, we have explored some representative hydrogen-bond catalysts under identical conditions to facilitate a direct comparison (Table 1). In contrast to the **C1** and **C1** / 18-crown-6 systems (Entries 1 and 2), representative non-covalent catalysts **NC1** and **NC2**, give no catalysis on their own, or with 18-crown-6 (Entries 3-6). Adding the organic base DBU, which has a basicity (estimated pK_a of $DBUH^+$ is 12) sufficient to deprotonate **Nu1**H (pK_a = 5.7), to the H-bond catalysts does generate low yields of product (Entries 7 and 8). However, these yields are actually worse than when DBU is used on its own (Entry 9). To make another comparison, we have also added DBU to the **C1** catalyzed reaction (Entry 10). Unlike the small molecule H-bond catalysts, adding DBU to **C1** significantly improves reactivity compared to the individual catalysts (Entry 10 vs Entry 1 and Entry 9), giving close to quantitative yield in just 1 hour. This indicates two further points. First, it clearly shows that the 18-crown-6 is a highly efficient additive, giving a similar effect to a strong organic base (Entries 2 vs 10; see Figure S8 for kinetic profiles). In addition, the enhancement attained by adding **C1** to a reaction in which **Nu1**H would be deprotonated anyway (Entries 9 vs 10) would suggest that the cage plays a bigger role than just enhancing the acidity of the pro-nucleophile.

Table 1. Comparison of the C1 / 18-crown-6 with other non-covalent catalyst systems.

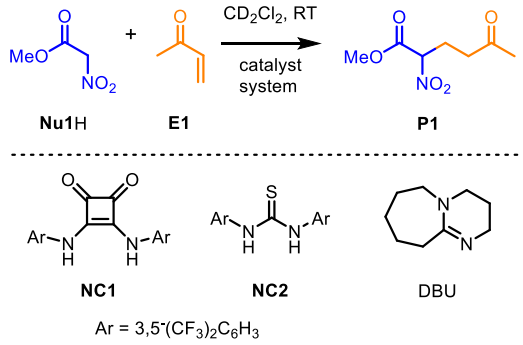

Entry	Catalyst system	% Yield (1 h)	% Yield (52 h)
1	**C1**	2	54
2	**C1** / 18-crown-6	≥ 98	≥ 98
3	**NC1**	No reaction	
4	**NC2**	No reaction	
5	**NC1** / 18-crown-6	No reaction	
6	**NC2** / 18-crown-6	No reaction	
7	**NC1** / DBU	1	38
8	**NC2** / DBU	0	15
9	DBU	2	44
10	**C1** / DBU	≥ 98	≥ 98

Conditions: **Nu1H** (12.5 mmol), **E1** (2.5 mmol), Cat (20 mol%), DBU (10 mol%), 18-crown-6 (2.5 mmol), CD_2Cl_2 (500 µL). Yields determined by ^{1}H NMR spectroscopy.

The cage promoted Michael addition reaction shows a surprisingly diverse substrate scope compared to other examples of confined microenvironment catalysis. With completely enclosed capsule-type assemblies, catalysis is highly dependent on the volume of the encapsulated substrates, intermediates and transition states.[19] In contrast, **C1** possesses a partially open structure with portals into which remote substituents can project. This also facilitates the kinetics of product-substrate turnover. While complementarity still plays a key role in the guest encapsulation with **C1**, it is not determined predominately by overall substrate size (although there are still limitations). Instead, the strength of binding is controlled by complementary polar interactions; guests with suitably positioned functional groups that can simultaneously interact with the cage's two H-bond donor pockets show the highest affinity (e.g. quinones). It is therefore interesting that several of the substrates would be considered poorly complementary for the cage because they possess relatively weak H-bond acceptor groups (e.g. esters, nitro, nitrile) that are incorrectly aligned for optimal binding (e.g. **Nu3H**, **Nu4**H, **Nu5**H). This contrasts many examples of cage catalysis, which are based on strong substrate binding.[8a-c,10a] Here we show exactly the opposite, with high-affinity reactants showing no reactivity (Scheme 1) whereas poorly interacting substrates deliver highly efficient catalysis (Scheme 3). This infers that complementarity is manifest in the recognition of key intermediates and/or TS, which is often considered the hallmark of enzyme catalysis.

Despite the more open cavity that facilitates a diverse substrate scope, **C1** can still exhibit the types of interesting selectivity that have often characterized catalysis within enclosed systems. In this case, our attention was drawn to the catalytic formation of **P5** because the ^{1}H NMR spectrum was relatively simple considering the formation of three contiguous stereocenters, which corresponds to four pairs of diastereoisomers (Figure 2a,b). Indeed, this reaction exhibits complete selectivity for just the two *anti*-isomers, **P5a-b**. For comparison, the same reaction was carried out but using DBU in place of **C1** / 18-crown-6. The ^{1}H NMR spectrum of this reaction showed the expected formation of all four *syn* and *anti*-product diasteriomers, **P5a-d**, in an approximately equimolar ratio (Figure 2a,b).

To investigate this selectivity, a ^{1}H NMR titration between **C1** and **P5a-d** was carried out (Figure 2c). Due to the difficulty in separating the diastereomers, this experiment was conducted qualitatively with the mixture of all four isomers obtained from the DBU-only mediated process. Adding increasing amounts of **C1** to **P5a-d** reveals shifts in both the characteristic internal H-bond donor signal of the cage and the product H_a cyclohexyl resonances, confirming the formation of host-guest complexes (Figure 2c). Significantly, the signals of the *anti*-isomers **P5a-b** show the largest shift and one of the *syn*-isomer resonances moves noticeably less (Figure 2c, signal at ca. 4.97), which indicates that the cage can differentiate the *syn* and *anti*-diastereomeric products. Calculations at the SMD(DCM)-M06-2X/def2-TZVP//PBE0-D3BJ/def2-SVP level of theory with the individual isomers agree with the qualitative titration data (See Supporting Information, section 6). We have also investigated whether the *syn* and *anti*-isomers interconvert under catalytic conditions to ascertain whether stereoselectivity is an actual thermodynamic effect. This was done by repeating the same catalysis but adding a small quantity of the *syn* and *anti*-product mixture shortly after the reaction starts. The *syn* isomer concentrations in this experiment remain unchanged (see Figure S57) showing that the diastereospecificity is kinetically rather than thermodynamically controlled. However, the preferential binding of isomers **5a-b** still show that the cage cavity is capable stereospecific differentiation, it is just that diastereoselectivity is not caused by product recognition.

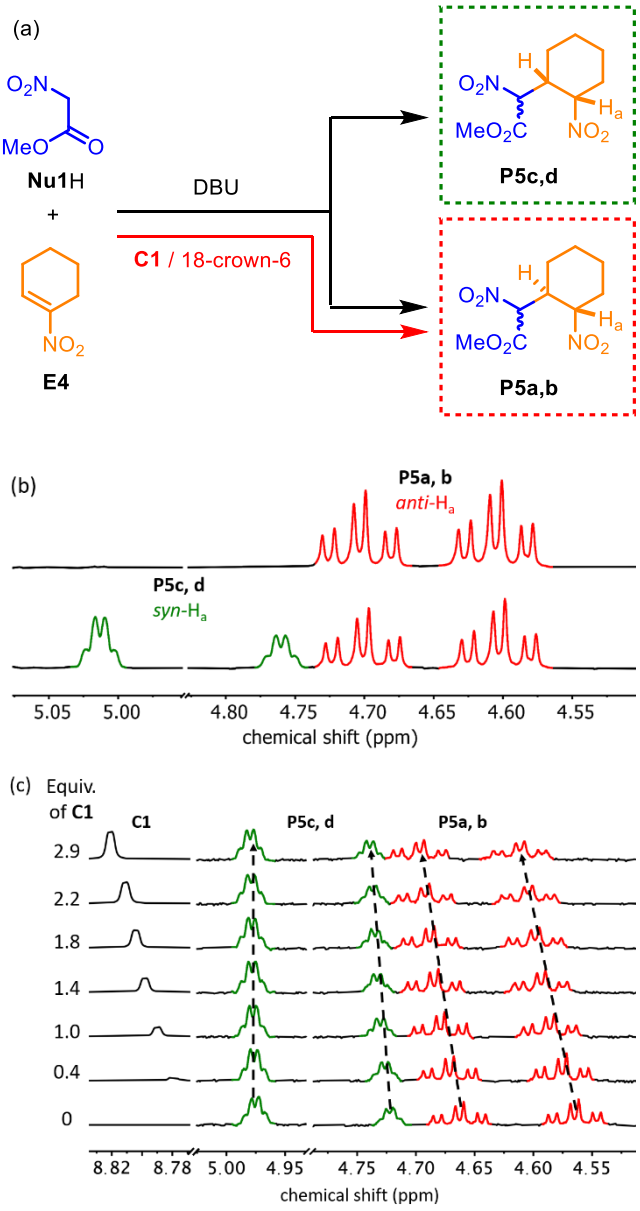

Figure 2. Stereoselective cage catalysis. (a) The DBU catalyzed formation of **P5** give all four diastereomers, **P5a-d** whereas **C1** produces only the pair of *anti*-diastereoisomers **P5a,b**. **(b)** The Partial ^{1}H NMR spectra (CD_2Cl_2, 500 MHz) of reaction mixtures for **C1** / 18-crown-6 (top) and DBU (bottom) catalyzed reactions. The *syn*- and *anti*-diastereomers are colored green and red. **(c)** Partial ^{1}H NMR spectra (CD_2Cl_2, 600 MHz) for the titration of **C1** into diastereomers **P5a-d**. The **C1** signals corresponds to the inward facing *o*-pyridyl proton. The intensity of the **C1** signal has been normalized to match the resonances of **P5a-d**.

To probe what appears to be a kinetic effect, we have carried out further calculations, focusing efforts on modelling the initial anionic intermediate, **P5-I1**$^-$ (Figure 3; see Supporting Information, section 6). This intermediate can exist as epimeric diastereomers, wherein the two newly formed stereogenic

centers possess either the same (*i.e.*, RR/SS) or opposite (*i.e.*, RS/RS) configurations. Furthermore, each diastereomer can exist in two distinct conformations, with the nitroester-methine group in either the pseudo-axial or equatorial positions. In the absence of the cage, the two conformations of both diastereomers are similar in energy, separated by 3.5 kcal mol^{-1}. In contrast, the range of relative energies of the four encapsulated species (pseudo-axial and equatorial conformations for both diastereomers) is a much larger 12.8 kcal mol^{-1}. There is also a pronounced bias (5 kcal mol^{-1}) towards one of the diastereomers with a pseudo-axial conformation. This conformation positions the acidic α-proton of the nitroester-methine group such that it can undergo a stereospecific intramolecular proton transfer, likely mediated by water.[20] This mechanism would deliver the proton to the same face (Figure 3, bottom) generating the *anti*-cyclohexyl stereochemistry in intermediate **P5-I2**$^-$ (Figure 3, top), which goes on to give the *anti*-stereochemistry observed in the product. This intramolecular proton transfer also erases the acyclic stereogenic center that arises in the C-C bond forming step. The generation of both *anti*-product isomers indicates that the final intermolecular proton transfer is not stereospecific.

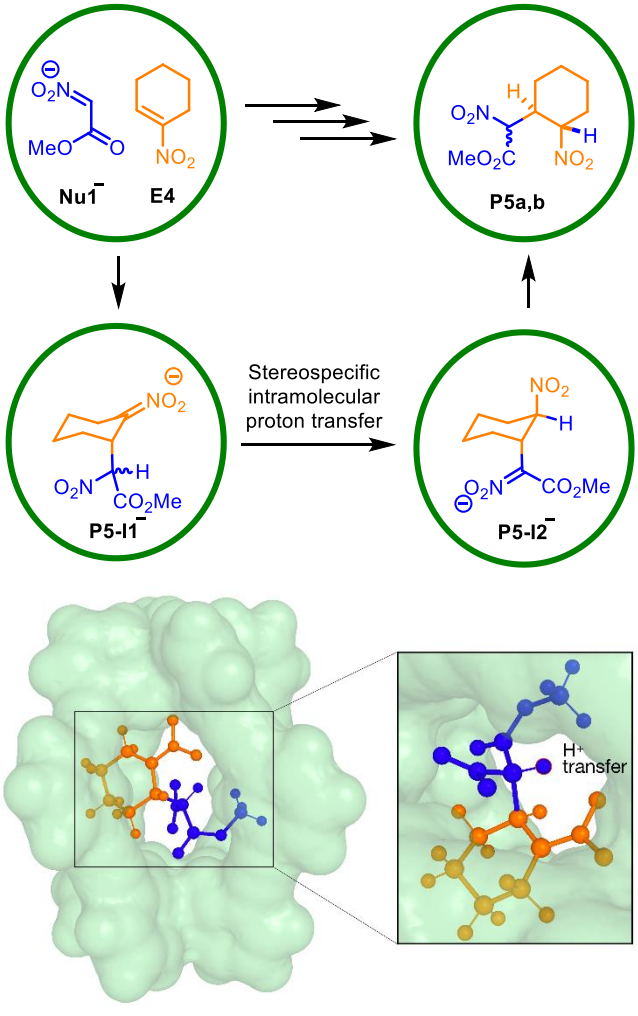

Figure 3. Stereoselective catalytic pathway. Top: An initial intramolecular proton-transfer would generate the observed anti-diastereoselectivity. Bottom: Most stable encapsulated diastereomeric conformer of P5-I1$^-$ calculated at the SMD(DCM)-M06-2X/def2-TZVP//PBE0-D3BJ/def2-SVP level of theory.

Conclusions

We have successfully demonstrated that a simple cationic coordination cage can be utilized to catalyze a chemical transformation by stabilizing anionic intermediates. Despite the simplicity of this concept, the lack of similar examples marks this out as a significant step forward in cage catalyzed methods. Moreover, synergizing the anion-stabilizing properties of the cage with the cation-stabilizing properties of a crown ether has facilitated a non-covalent method that is highly active and versatile. Catalysis also occurs without the functionality that is considered a pre-requisite for this type of reactivity (e.g. Brønsted base, Lewis Acid) making the method extremely mild. This form of charge-separated catalysis, built on compartmentalization of incompatible intermediates, could play a significant role in the development of new non-covalent approaches.

There remains several open questions regarding how the cage operates so efficiently. First, the remarkable reactivity can only be partly attributed to acidity enhancement as several strong-binding pro-nucleophiles show no catalysis. Instead catalysis only occurs when a weak-binding pro-nucleophile is combined with a small, weakly interacting electrophile, which would suggest that dual-activation is key. Cage catalysis that does not involve strongly bound substrates is still not a common strategy, yet this and other pioneering studies show that complementarity towards key intermedies (and ideally TS) should be the primary consideration.[3-6,21] The other side of catalytic efficiency – turnover – can also still be considered a challenge for many cage-catalyzed methods. This is particularly true for the catalysis of transformations that involve the fusion of smaller fragments, as is the case here. However, we observe efficient turnover even though it likely involves single product displacement by two very weakly binding substrates. Further studies are currently underway designed to shed light on these fundamental questions, which could ultimately lead to the development of new non-covalent catalysts that possess enzyme-like efficiencies.

Experimental Methods

General. All reagents and solvents were purchased from Alfa Aesar, VWR, Sigma Aldrich or Fluorochem. Column chromatography was carried out using Geduran Si60 (40-63 μm) as the stationary phase and TLC was performed on pre-coated Kieselgel 60 plates (0.20 mm thick, 60F254. Merck, Germany) and observed under UV light at 254 nm. All substrates and reagents were purified prior to use: **E1**, **E2**, **E3**, **E4** and **Nu3H** were purified by distillation; **Nu1H** and **Nu4H** were purified by silica plug (eluent: CH_2Cl_2); **Nu2H** and **Nu5H** were recrystallized from ^{i}PrOH; 18-crown-6 was purified by sublimation. Cage **C1** was prepared using the previously reported method.[9d] All reactions were carried out under air and at room temperature, unless otherwise stated.

All ^{1}H and ^{13}C NMR spectra were recorded on either a a 400 MHz BrukerAV III equipped with BBFO+ probe (Ava400), a 500 MHz Bruker AV III equipped with a DCH cryo-probe (Ava500), a 500 MHz Bruker AV IIIHD equipped with a Prodigy cryo-probe (Pro500) or a 600 MHz Bruker AV IIIHD equipped with a TCI cryo-probe (Ava600) at a constant temperature of 300 K. Chemical shifts are reported in parts per million. Coupling constants (J) are reported in hertz (Hz). Apparent multiplicities are reported using the following standard

abbreviations: m = multiplet, q = quartet, t = triplet, d = doublet, s = singlet. All analysis was performed with MestReNova, Version 14.0.0. All assignments were confirmed using a combination of COSY, NOESY, HMBC and HSQC NMR spectra.

General Procedure for C1 / Crown ether catalyzed Michael addition. To an NMR tube was introduced a solution containing the cage compound (450 µL of a 0.56 mM CD_2Cl_2 stock solution), the Michael donor (20 µL of a 312.5 mM CD_2Cl_2 stock solution), the Michael acceptor (10 µL of a 125 mM CD_2Cl_2 stock solution), and the internal standard tetrakis(trimethylsilyl)silane (10 µL of a 15.6 mM CD_2Cl_2 stock solution). The Michael addition was started by the addition of 18-crown-6 (10 µL of a 125 mM CD_2Cl_2 stock solution). All the reactions were kept at 298 K and ^{1}H NMR spectra were recorded at regular intervals. Kinetic NMR data were processed using the MestreNova 14.0.0 software and the concentrations of all chemical species were determined using NMR integration against the internal standard at each reaction time point.% yield was calculated when no further change occurred.

Preparative scale formation of P1 using the C1 / Crown ether catalyzed Michael addition method. Nitromethey-lacetate (75 mg, 0.63 mmol) and methyl vinyl ketone (33.1 mg, 0.42 mmol) were combined in CH_2Cl_2 (70 ml). **C1** (40 mg, 8.4 µmol, 2 mol%) and 18-crown-6 (11.1 mg, 42 µmol, 10 mol%) were added to the mixture. The reaction was stirred at room temperature for 44 hours then concentrated *in vacuo*. The residual pale yellow oil was purified by column chromatography (CH_2Cl_2, R_f = 0.28), yielding colorless oil (72.4 mg, 91%). ^{1}H NMR (500 MHz, $CDCl_3$) δ 5.22 (dd, J = 8.4, 6.1 Hz, 1H), 3.79 (s, 3H), 2.65 – 2.50 (m, 2H), 2.48 – 2.34 (m, 2H), 2.12 (s, 3H). ^{13}C NMR (126 MHz, $CDCl_3$) δ 206.06, 164.85, 86.63, 53.65, 38.31, 29.91, 24.10. HRMS (EI): $C_7H_{11}NO_5$ $[M]^{\cdot+}$ found 189.06235, calculated 189.06317.

ASSOCIATED CONTENT

Supporting Information

The Supporting Information is available free of charge on the ACS Publications website. This includes details of all catalytic experiments, kinetic data, titration data and characterization of all products.

AUTHOR INFORMATION

Corresponding Author

Paul.Lusby@ed.ac.uk

fernanda.duartegonzalez@chem.ox.ac.uk

Notes

The authors declare no competing financial interests.

ACKNOWLEDGMENT

We acknowledge the University of Edinburgh for a Principal's Career Development and Edinburgh Global Research Scholarships for JW, and the EPSRC Theory and Modelling in Chemical Sciences Doctoral training Centre (EP/L015722/1) for a studentship to TAY, generously supported by AWE.

REFERENCES

(1) (a) Warshel, A.; Sharma, P. K.; Kato, M.; Xiang, Y.; Liu, H.; Olsson, M. H. M. Electrostatic Basis for Enzyme Catalysis. *Chem. Rev.* **2006**, *106*, 3210.

(2) (a) Knowles, R. R.; Jacobsen, E. N. Attractive noncovalent interactions in asymmetric catalysis: links between enzymes and small molecule catalysts. *Proc. Natl Acad. Sci.* **2010**, *107*, 20678. (b) Neel, A. J.; Hilton, M. J.; Sigman, M. S.; Toste, F. D.Exploiting non-covalent π interactions for catalyst design. Nature, **2017**, *543*, 637. (c) Davis, H. J.; Phipps, R. J. Harnessing non-covalent interactions to exert control over regioselectivity and site-selectivity in catalytic reactions. *Chem. Sci.* **2017**, *8*, 864–877.

(3) Pluth, M. D.; Bergman, R. G.; Raymond, K. N. Acid Catalysis in Basic Solution: A Supramolecular Host Promotes Orthoformate Hydrolysis. *Science* **2007**, *316*, 85.

(4) Bierschenk, S. M.; Bergman, R. G.; Raymond, K. N.; Toste, F. D. A Nanovessel-Catalyzed Three-Component Aza-Darzens Reaction. *J. Am. Chem. Soc.* **2020**, *142*, 733.

(5) (a) Hastings, C. J.; Pluth, M. D.; Bergman, R. G.; Raymond, K. N. Enzymelike Catalysis of the Nazarov Cyclization by Supramolecular Encapsulation. *J. Am. Chem. Soc.* **2010**, *132*, 6938.

(6) Kaphan, D. M.; Levin, M. D.; Bergman, R. G.; Raymond, K. N.; Toste, F. D. A supramolecular microenvironment strategy for transition metal catalysis. *Science* **2015**, *350*, 1235.

(7) (a) Chakrabarty, R.; Mukherjee, P. S.; Stang, P. J. Supramolecular Coordination: Self-Assembly of Finite Two- and Three-Dimensional Ensembles. *Chem. Rev.* **2011**, *111*, 6810. (b) Cook, T. R.; Stang, P. J. Recent Developments in the Preparation and Chemistry of Metallacycles and Metallacages via Coordination. *Chem. Rev.* **2015**, *115*, 7001. (c) Sun, Y.; Chen, C.; Liuc, J.; Stang, P. J. Recent developments in the construction and applications of platinum-based metallacycles and metallacages via coordination. *Chem. Soc. Rev.* **2020**, *49*, 3889 (d) Clever, G. H.; Tashiro, S.; Shionoya, M. Inclusion of Anionic Guests inside a Molecular Cage with Palladium(II) Centers as Electrostatic Anchors. *Angew. Chem. Int. Ed.* **2009**, *48*, 7010. (e) Liao, P.; Langloss, B. W.; Johnson, A. M.; Knudsen, E. R.; Tham, F. S.; Julian, R. R.; Hooley, R. J. Two-component control of guest binding in a self-assembled cage molecule. *Chem. Commun.* **2010**, *46*, 4932. (f) Lewis, J. E. M.; Gavey, E. L.; Cameron, S. A.; Crowley, J. D. Stimuli-responsive Pd_2L_4 metallosupramolecular cages: towards targeted cisplatin drug delivery. *Chem. Sci.* **2012**, *3*, 778. (g) Bloch, W. M.; Holstein, J. J.; Hiller, W.; Clever, G. H. Morphological Control of Heteroleptic *cis*- and *trans*-$Pd_2L_2L''_2$ Cages. *Angew. Chem. Int. Ed.* **2017**, *56*, 8285. (h) Lewis, J. E. M.; Tarzia, A.; White, A. J. P. Jelfs, K. E. Conformational control of Pd_2L_4 assemblies with unsymmetrical ligands. *Chem. Sci.* **2020**, *11*, 677.

(8) (a) Murase, T.; Nishijima, Y.; Fujita, M. Cage-Catalyzed Knoevenagel Condensation under Neutral Conditions in Water *J. Am. Chem. Soc.* **2011**,*134*, 162. (b) Bolliger, J. L.; Belenguer, A. M.; Nitschke, J. R. Enantiopure water-soluble $[Fe_4L_6]$ cages: host-guest chemistry and catalytic activity. *Angew. Chem. Int. Ed.* **2013**, *52*, 7958. (c) Cullen, W.; Misuraca, M. C.; Hunter, C. A.; Williams, N. H.; M. D. Ward. Highly efficient catalysis of the Kemp elimination in the cavity of a

cubic coordination cage. *Nat. Chem.* **2016**, *8*, 231. (d) Taylor, C. G. P.; Metherell, A. J.; Argent, S. P.; Ashour, F. M.; Williams, N. H.; Ward, M. D. Coordination-Cage-Catalysed Hydrolysis of Organophosphates: Cavity- or Surface-Based? *Chem. Eur. J.* **2020**, *26*, 3065.

(9) (a) Zhao, Y.; Domoto, Y.; Orentas, E.; Beuchat, C.; Emery, D.; Mareda, J.; Sakai, N.; Matile, S. Catalysis with Anion-π Interactions. *Angew. Chem., Int. Ed.* **2013**, *52*, 9940–9943. (b) Zhao, Y.; Cotelle, Y.; Liu, L.; López-Andarias, J.; Bornhof, A.-B.; Akamatsu, M.; Sakai, N.; Matile, S. The Emergence of Anion-π Catalysis. *Acc. Chem. Res.* **2018**, *51*, 2255. (c) López-Andarias, J.; Frontera, A.; Matile, S. Anion−π Catalysis on Fullerenes. *J. Am. Chem. Soc.* **2017**, *139*, 13296.

(10) (a) Martí-Centelles, V.; Lawrence, A. L.; Lusby, P. J., High Activity and Efficient Turnover by a Simple, Self-Assembled "Artificial Diels–Alderase". *J. Am. Chem. Soc.* **2018,** *140*, 2862. (b) Young, T. A.; Martí-Centelles, V.; Wang, J.; Lusby, P. J; Duarte, F. Rationalizing the Activity of an "Artificial Diels-Alderase": Establishing Efficient and Accurate Protocols for Calculating Supramolecular Catalysis. *J. Am. Chem. Soc.* **2020**, 142, 1300. (c) Spicer, R. L.; Stergiou, A. D.; Young, T. A.; Duarte, F.; Symes, M. D.; Lusby, P. J. *J. Am. Chem. Soc.* **2020**, 142, 2134. (d) August, D. P.; Nichol, G. S.; Lusby, P. J. Maximizing Coordination Capsule–Guest Polar Interactions in Apolar Solvents Reveals Significant Binding. *Angew. Chem. Int. Ed.* **2016**, *55*, 15022. (e) All association constants measured in dichloromethane.

(11) (a) Rideout, D. C.; Breslow, R. Hydrophobic acceleration of Diels-Alder reactions. *J. Am. Chem. Soc.* **1980**, *102*, 7817. (b) Kang, J.; Rebek Jr., J. Acceleration of a Diels–Alder reaction by a self-assembled molecular capsule. *Nature* **1997**, *385*, 50. (c) Yoshizawa, M.; Tamura, M.; Fujita, M. Diels-Alder in Aqueous Molecular Hosts: Unusual Regioselectivity and Efficient Catalysis. *Science* **2006**, *312*, 251. (d) Fiedler, D.; Bergman, R. G.; Raymond, K. N. Supramolecular Catalysis of a Unimolecular Transformation: Aza-Cope Rearrangement within a Self-Assembled Host. *Angew. Chem., Int. Ed.* **2004**, *43*, 6748.

(12) Okino, T.; Hoashi, Y.; Takemoto, Y. Enantioselective Michael Reaction of Malonates to Nitroolefins Catalyzed by Bifunctional Organocatalysts. *J. Am. Chem. Soc.* **2003**, *125*, 12672.

(13) Evans, D. A.; Seidel, D. Ni(II)-Bis[(*R*,*R*)-*N*,*N*'-dibenzylcyclohexane-1,2-diamine]Br_2 Catalyzed Enantioselective Michael Additions of 1,3-Dicarbonyl Compounds to Conjugated Nitroalkenes. *J. Am. Chem. Soc.* **2005**, *127*, 9958.

(14) Attempts to remove water from the catalyzed reaction have been hampered by the poor solubility of **C1** in anhydrous dichloromethane.

(15) Guideri, L.; De Sarlo, F.; Machetti, F. Conjugate Addition versus Cycloaddition/Condensation of Nitro Compounds in Water: Selectivity, Acid–Base Catalysis, and Induction Period. *Chem. Eur. J.* **2013**, *19*, 665.

(16) Wang, K.; Cai, X.; Yao, W.; Tang, D.; Kataria, R.; Ashbaugh, H. S.; Byers, L. D.; Gibb, B. C. Electrostatic Control of Macrocyclization Reactions within Nanospaces. *J. Am. Chem. Soc.* **2019**, *141*, 6740.

(17) Atwood, J. L.; Bott, S.G.; Means, M.; Coleman, A. W.; Zhang, H.; May, M. T. Synthesis of Salts of the Hydrogen Dichloride Anion in Aromatic Solvents. 2. Syntheses and Crystal Structures of [K·18-crown-6][Cl-H-Cl], [Mg·18-crown-6][Cl-H-Cl]$_2$, [$H_3$0·18-crown-6][Cl-H-Cl], and the Related [$H_3$0·18-crown-6][Br-H-Br]. *Inorg. Chem.* **1990**, *29*, 467.

(18) (a) Trogu, E.; De Sarlo, F.; Machetti, F. Michael Additions versus Cycloaddition Condensations with Ethyl Nitroacetate and Electron-Deficient Olefins. *Chem. Eur. J.* **2009**, *15*, 7940. (b) Martínez, J. I.; Villar, l; Uria, U.; Carrillo, L.;, Reyes, E.; Vicarioa, J. L. Bifunctional Squaramide Catalysts with the Same Absolute Chirality for the Diastereodivergent Access to Densely Functionalised Cyclohexanes through Enantioselective Domino Reactions. Synthesis and Mechanistic Studies. *Adv. Synth. Catal.* **2014**, *356*, 3627.

(19) Mecozzi, S.; Rebek, J. The 55 % Solution: A Formula for Molecular Recognition in the Liquid State. *Chem. Eur. J.* **1998**, *4*, 1016.

(20) Due to the difficulties in identifying the TS for intramolecular proton transfer within the cage (because of greater than 150 atoms), we have modelled the non-bound reaction (see Supporting Information, section 6). This shows that a water mediated mechanism is a relatively low energy process (21.7 kcal mol^{-1}) commensurate with the observed reaction times.

(21) Merget, S.; Catti, L.; Piccini, G. M.; Tiefenbacher K. Requirements for Terpene Cyclizations inside the Supramolecular Resorcinarene Capsule: Bound Water and its Protonation Determine the Catalytic Activity. *J. Am. Chem. Soc.* **2020**, *142*, 4400.

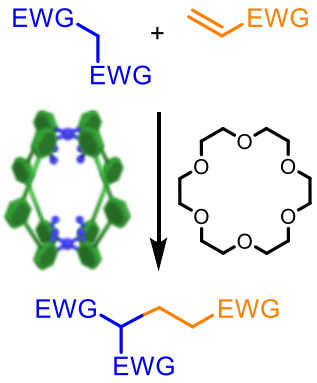

+ Non-covalent activation of pro-nucleophiles under base-free conditions

+ High activity and effecient turnover

+ Wide substrate scope - despite enclosed reactivity

+ High stereoselectivity